

Correlating DMS Simulations with Experiments

Frank Londry¹; Bradley B. Schneider¹; Erkinjon G. Nazarov²; Thomas R. Covey¹
¹AB SCIEX, 71 Four Valley Drive, Concord, ON, L4K 4V8 Canada; ²Draper Laboratories Bioengineering Center, Tampa, FL, USA

INTRODUCTION

This poster describes advances in simulations of ion motion in a DMS instrument. The simulator combines computational fluid dynamics (CFD) solutions for the gas flows and temperature profiles with electrostatic solutions for all of the applied potentials in a DMS/MS interface. The simulator has proven to be a useful tool for furthering instrument design optimization. The first section of the poster proposes a new method of determining alpha curves from experimental DMS data, and then provides verification of the alpha curves and simulator by comparison to experimental CoV data. The second section of the poster demonstrates use of the simulator to improve DMS design.

MATERIALS AND METHODS

Experimental verification of the modeling results were generated using a hybrid triple quadrupole/linear ion trap mass spectrometer with a prototype DMS system. CFD solutions for this system were provided by Metacomp, using boundary temperature conditions that were measured on the prototype DMS/MS interface. Laplace solutions were obtained using the Rx solver, which was developed in-house and uses successive over-relaxation to obtain the potential on a three-dimensional Cartesian grid. Trajectories were calculated using another in-house package, the Sx simulator. Sx interpolates and superposes Laplace solutions and generates trajectories by integrating the equations of motion numerically.

Results

Part One: Determination of Alpha and Verification of the Simulator

The field dependent mobility behavior for an ion in DMS is characterized by its alpha function, as defined in Equation 1, where $K(E)$ is the ion mobility at a particular field, and $K(0)$ is the low field mobility.

$$\alpha(E) = \frac{K(E) - K(0)}{K(0)} \quad \text{Equation 1}$$

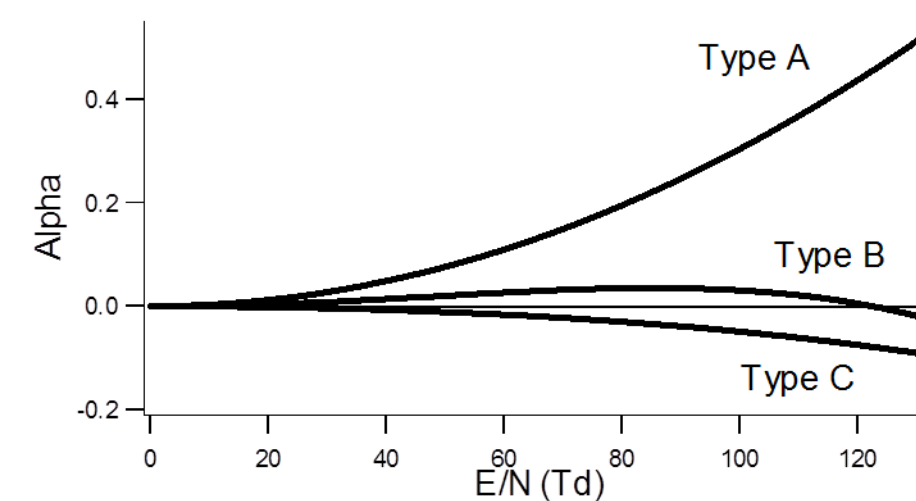


Figure 1. General shapes for alpha curves

Alpha can be expanded as a function of the separation field (S) in DMS, as shown in Equation 2.

$$\alpha(S) = \alpha_2 S^2 + \alpha_4 S^4 + \alpha_6 S^6 + \alpha_8 S^8 + \dots \quad \text{Equation 2}$$

The compensation field (C) in DMS can be evaluated as shown in Equation 3 [Buryakov et al, 1993].

$$C = \frac{-\langle S\alpha(S) \rangle}{1 + \langle \alpha(S) \rangle + \langle S\alpha'(S) \rangle} \quad \text{Equation 3}$$

The terms $\langle \alpha(S) \rangle$, $\langle S\alpha(S) \rangle$, and $\langle S\alpha'(S) \rangle$ can be evaluated as shown in Equations 4-6.

$$\langle \alpha(S) \rangle = \frac{1}{T} \int_0^T \alpha(S(t)) dt \quad \text{Equation 4} \quad \langle S\alpha(S) \rangle = \frac{1}{T} \int_0^T S(t) \alpha(S(t)) dt \quad \text{Equation 5} \quad \langle S\alpha'(S) \rangle = \frac{1}{T} \int_0^T S(t) \alpha'(S(t)) dt \quad \text{Equation 6}$$

Therefore, it is possible to determine the alpha function for an ion by adjusting the coefficients of Equation 2 to obtain an alpha function that gives the best fit to experimental data by Equation 3. This approach has been utilized for ions exhibiting Type A, B, and C behaviors, and we have generally found that alpha functions calculated in this manner are accurate provided that at least 3 terms are utilized in Equation 2.

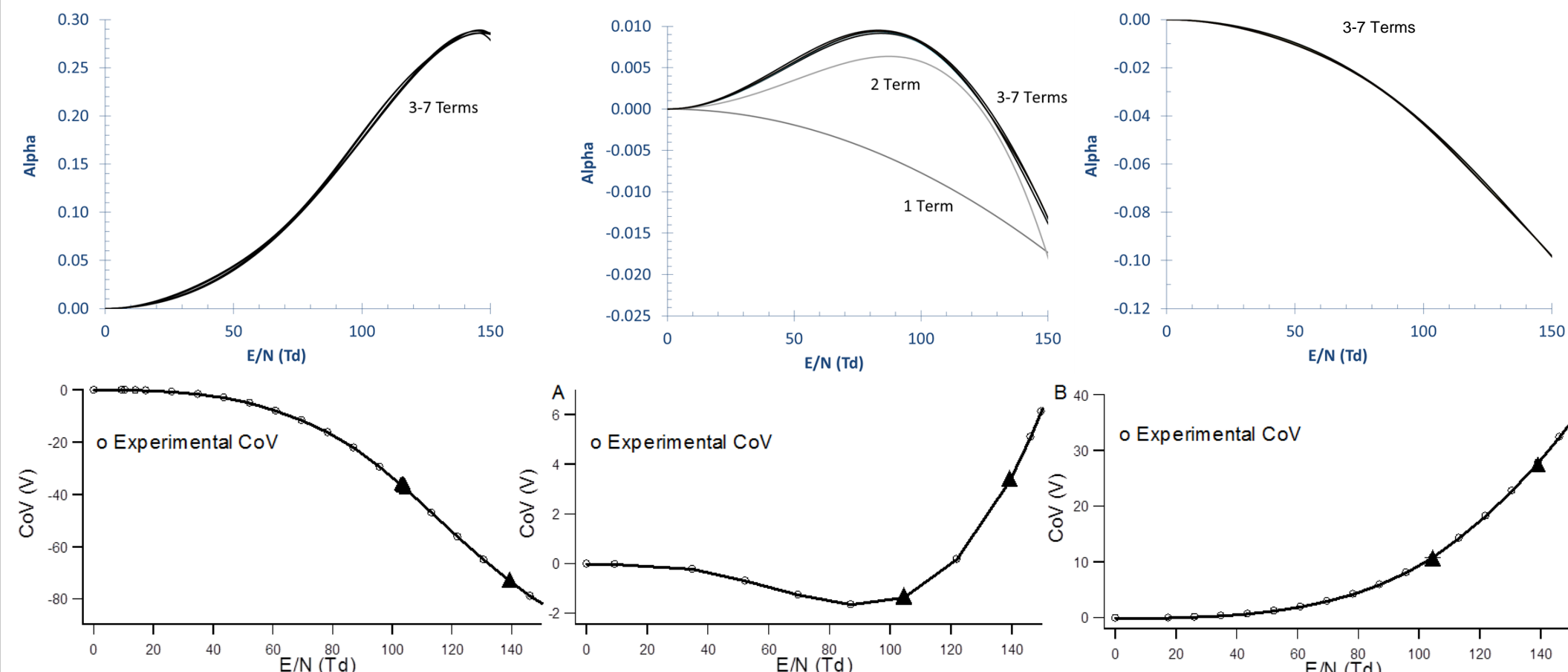


Figure 2. Alpha curves determined from experimental data (top panes) for ions exhibiting Type A, B, and C behavior (left to right), and experimental CoV curves for the same ions (bottom panes) with overlays of the center of simulated ionograms from the Sx simulator, using the alpha data from above. The simulated points are included as triangles in the above plots.

The data presented in Figure 2 demonstrate good agreement between experimental CoV values and simulated CoV values using the Sx simulator with experimentally derived alpha curves. These data are important because they confirm the integrity of the simulator, an important first step prior to using the simulator for design optimization.

Part Two: Experimental Data and Simulations of the Importance of Homogeneous E/N for modifier separations.

A) Homogeneous vs Inhomogeneous Temperatures

It has been demonstrated previously that the critical parameter affecting the magnitude of the CoV in DMS separations is the E/N ratio, or the separation field/gas number density [Krylov et al., 2009], usually presented in Townsend units (Td). The temperature of the transport gas directly affects the E/N ratio and therefore, the optimal CoV. Figure 3a shows experimental data for methylhistamine ions under cluster/decluster conditions in a DMS, taken with a 21° C temperature gradient from the front to the back of the cell (ionogram 1), and under conditions where the temperature gradient is reduced to 1° C (ionogram 4). Ionograms 2 and 3 show intermediate conditions. Establishment of a homogeneous E/N increases the signal and reduces the peak width. Figure 3b shows a simulation of the 21° C temperature gradient for the collection of ionogram 1. In addition to reduced transmission, inhomogeneous E/N ratios broadened the ionogram from 1.17 V to 1.74 V FWHM.

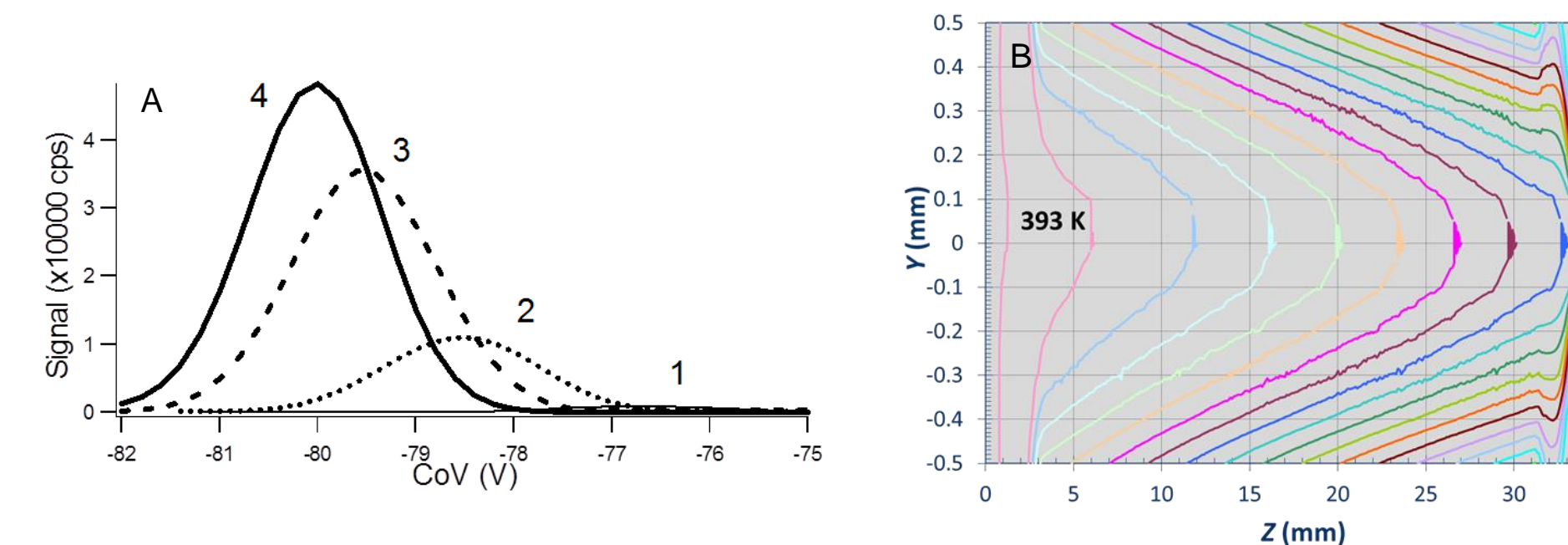


Figure 3 A) Ionograms taken with DMS temperature gradients from 21° C (plot 1) to 1° C (plot 4). B) Contours of constant temperature from a CFD solution of the experimental conditions of panel A.

Ion losses in DMS occur when the E/N is inhomogeneous due to a reduction of the effective gap. Figure 4 shows a simulated ion trajectory when the inhomogeneity of E/N was caused by a large temperature gradient (4a) and a simulated ion trajectory when E/N was homogeneous (no temperature gradient). In both cases, there is some deflection of the ion in the inlet fringing field (Z = 3-4 mm). In the case of the homogeneous field condition, the CoV balances the SV, and the ion travels approximately straight through the cell (4b). However, when the fields are inhomogeneous, the CoV initially undercompensates (Z = 5-10 mm), and then overcompensates (Z = 10 – 30 mm), causing the ion to be substantially displaced from the central axis. The separation E/N ratios experienced by the ions are shown in Figures 5a (inhomogeneous field) and 5b (homogeneous field).

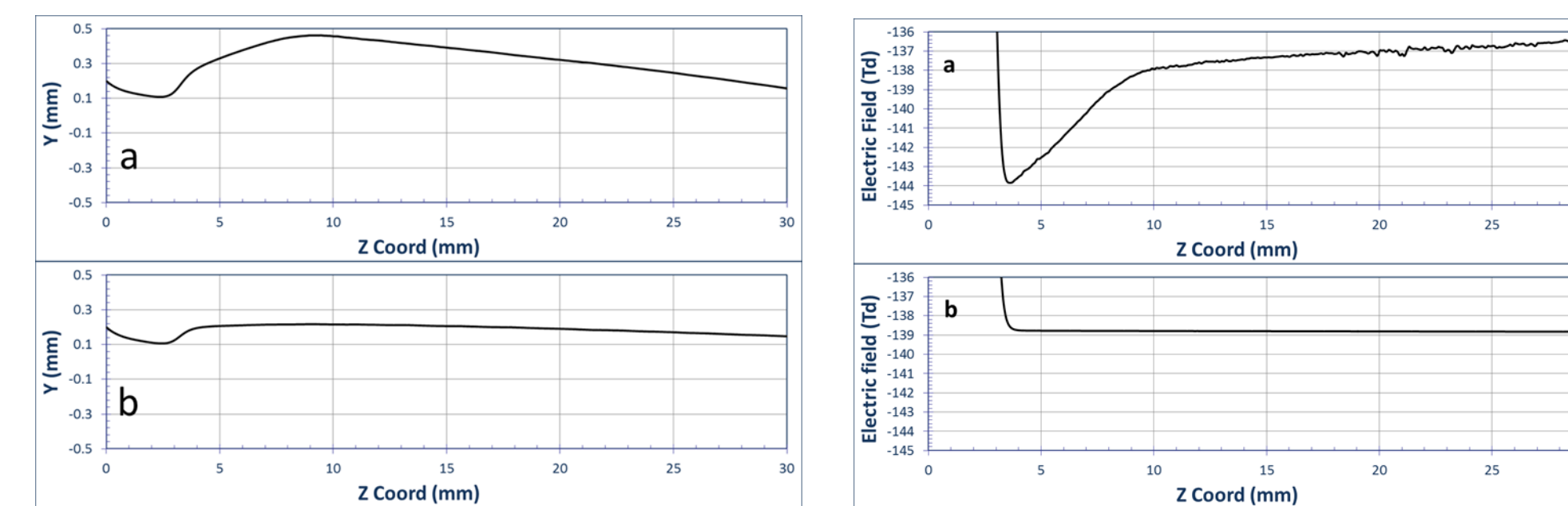


Figure 4. Ion trajectory simulations with inhomogeneous fields (a) and homogeneous fields (b). Figure 5. Separation E/N ratios for the trajectories shown in Figure 4.

B) Homogeneous vs Inhomogeneous Fields

The results presented in Figure 3a demonstrate the importance of homogeneous E/N ratios for DMS separations in the presence of chemical modifiers. Curved geometry (FAIMS) devices establish inhomogeneous fields within the analyzer. These effects can be partially compensated by temperature gradients, however, much like the data shown in Figure 3, the peak width will be affected. Figure 6 shows a reproduction of previously published data showing the separation of a group of 5 chemicals using a device with inhomogeneous electric fields without modifiers (top pane) and with different modifier concentrations (bottom panes) [Purves et al., 2014]. The same separation is shown using the lowest resolution setting of a DMS system operating with homogeneous E/N ratio, in Figure 7. Figure 8 shows the same separation using an intermediate resolution setting from a DMS system operating with homogeneous E/N ratio. In each case, the peak capacity was approximated as the spread of the peaks/average FWHM. The ionograms correspond to betaine (green), choline (blue), GABA (black), alanine (red), and acetaminophen (grey).

In the case of the FAIMS device, the peak spread increased by a factor of up to 6.5 when modifiers were present. However, the average peak width also increased by ~ 3.7X as a result of the inhomogeneous E/N ratio. Therefore, the peak capacity improvement was limited to 1.7X. Additional increases in modifier concentration (up to 3%) degraded peak capacity further. The DMS device used 3% acetonitrile, where best performance was observed. In the case of the DMS device, peak width was relatively unaffected by the presence of the clustering agent, and the peak capacity improvement (~3.6X) scaled with the increased peak spread. These results demonstrate the benefits of homogeneous E/N when using modifiers with DMS or FAIMS devices. Under maximum peak capacity conditions, the resolution for choline was approximately 7.6, 68, and 145 for the FAIMS device, low resolution DMS, and medium resolution DMS, respectively.

PC

5.5
8.1
9.4
7.3

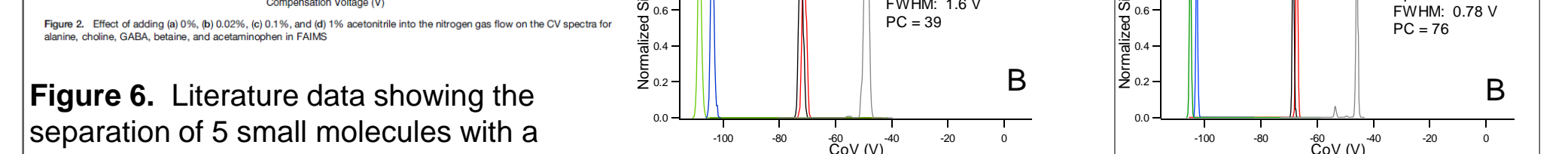


Figure 6. Literature data showing the separation of 5 small molecules with a FAIMS device and no ACN modifier (top pane) and the addition of different amounts of ACN modifier (bottom panes) [Purves et al., 2014]. (reprinted with kind permission from Springer Science and Business Media).

CONCLUSIONS

- The Sx simulator combines CFD solutions for gas flows and temperature profiles with electrostatic solutions for all of the potentials in a DMS/MS interface.
- The integrity of the simulator has been verified by comparison of simulated and experimental ionograms.
- This simulator presents a useful tool for instrument design optimization, and has been used to verify the importance of uniform E/N for chemically modified separations.

REFERENCES

- Guevremont R & Purves RW, Rev. Sci Instr., 1999, 70, 1370-1383.
- Buryakov IA, Krylov EV, Nazarov EG, Rasulev Ukh, Int. J. Mass Spectrom. Ion Proc., 1993, 128, 143-148.
- Krylov EV, Coy SL, Nazarov EG, Int. J. Mass Spectrom., 2009, 279, 119-125.
- Purves RW, Ozog AR, Ambrose SJ, Prasad S, Belford M, Dunyach JJ, J. Am. Soc. Mass Spectrom., 2014, in press, DOI: 10.1007/s13361-014-0878-z.

TRADEMARKS/LICENSING

For Research Use Only. Not for use in diagnostic procedures. The trademarks mentioned herein are the property of AB Sciex Pte. Ltd. or their respective owners. AB SCIEX™ is being used under license. © 2014 AB SCIEX.

Figure 7. Experimental data taken for the same 5 small molecules as Figure 6 using ACN modifier with a low resolution DMS device (6.5 ms residence time) and homogeneous separation fields. A) Nitrogen transport gas and B) nitrogen with ACN modifier.

Figure 8. Experimental data taken for the same 5 small molecules as Figure 6 using ACN modifier with a medium resolution DMS device (13 ms residence time) and homogeneous separation fields. A) Nitrogen transport gas and B) nitrogen with ACN modifier.